

Magnetocaloric Effect in Copper Doped Ni_2MnIn

Jonathan Fee, Thomas Li, Andy Rodriguez, Casey Scoggins

Department of Physics, Miami University, Oxford, Ohio 45056, USA

May 18, 2018

Abstract

We experimented to discover the potential of copper doped Ni_2MnIn ($\text{Ni}_2\text{Mn}_{1-x}\text{Cu}_x\text{In}$) as a material to be used in magnetic refrigeration in order to increase the efficiency of future refrigerators. To do this we extensively experimented with our compound to see its properties. We first determined that the doping of copper has little to no noticeable effect on the body-centered cubic structure of our compound. Then after testing for various other properties of $\text{Ni}_2\text{Mn}_{1-x}\text{Cu}_x\text{In}$ for $x = 0, 0.05, 0.10, 0.15, 0.20$ various property changes were revealed. The Curie Temperature (T_C) over all values of x varied by 67 K, with the most promising being $x = 0.15$ with a T_C of 291 K. The refrigeration capacity at smaller magnetic fields of the material was increased for every compound that was doped in copper, with $x = 0.10$ showing the most promise. Hopefully with further testing $\text{Ni}_2\text{Mn}_{1-x}\text{Cu}_x\text{In}$ could show promise as a relatively cheap material to be used in magnetic refrigeration.

Introduction

Temperature controlling plays an increasingly significant role in various aspects of life. The most commonly used devices to achieve temperature control are refrigerators and air conditioners. Refrigeration is a \$36 billion industry and refrigeration and air conditioning are among the largest factors in worldwide energy consumption.¹ Predominant refrigeration relies heavily on the use of harmful refrigerants such as CFC, the extensive use of which has caused much damage to the Ozone layer. New temperature controlling methods that are free from chemical reliance have been researched extensively in the past few decades, one of which is to employ the magnetic-heat effects in certain alloys, known as the magnetocaloric effect.²³

The magnetocaloric effect (MCE) is the property of certain materials to experience a temperature change when subject to a changing magnetic field. It is describable through the second law of thermodynamics¹. By using a process comparable to the Carnot refrigeration cycle it is possible to use the magnetocaloric effect in creating magnetic refrigerators.² Through studying the MCE, we hope to find a way to make these magnetic refrigerators commercially viable. While some magnetic refrigerators are currently in employment, they are not accessible to the common consumer. The MCE was discovered in 1881 by Emil Warburg³. It had not drawn much research attention until the past few decades with the discovery of Gadolinium (Gd) exhibiting a strong MCE and having a Curie temperature near room temperature^{4,5}. The Curie temperature is the temperature at which the magnetic dipoles in ferromagnetic materials begin to align randomly. Gd is the only pure metal to have a Curie temperature near room temperature⁶. After further research, compounds such as $\text{Gd}_{1-x}\text{C}_x$ ($x = 0 - 0.025$), $\text{Gd}_{1-x}\text{B}_x$ ($x = 0 - 0.07$), and $\text{Gd}_5(\text{Si}_2\text{Ge}_2)$ were discovered to have a large MCE^{7,8,9}. However, while effective, Gd and Germanium (Ge) are both rare and expensive. We are searching for a more economically feasible compound that has a large MCE to use in magnetic refrigeration.

In order to make magnetic refrigeration commercially available, not only does the material need to be cheaper, it must also have a large MCE, a near room temperature Curie temperature, a good second order magnetostructural phase transition (SOMT) rather than first order (FOMT), and a high refrigeration capacity. This is a sought after characteristic because while FOMT materials exhibit larger MCE¹¹, changing physical structural properties during phase transitions leads to quick degradation of the material over repeated cycles¹². SOMT materials show no magnetic hysteretic behavior¹³ and experience no physical changes and little degradation over repeated cycles. While SOMT materials have lower changes in entropy, their refrigeration capacities are comparable. The importance of these values will be discussed later. The compound investigated in this paper consists of more common, cheaper materials: nickel, manganese, indium, and copper. Compounds of significantly cheaper and less rare materials are vital to commercializing and exploring the MCE. Ni_2MnIn by itself has a Curie temperature of 315 K, which is close to room temperature, and has a reasonable MCE. We are interested in studying the effects of Copper doping Ni_2MnIn to see if we can find a greater MCE that is still has a transition temperature near room temperature.

Experimental Techniques

2g buttons of each compound were created via arc melting and annealing processes. Stoichiometric calculations were performed to determine the elements needed for each compound for $0 \leq x \leq 0.25$ (Table 1). Elements were obtained from Alfa Aesar Inc. and had more than 3N purity. The arc melting apparatus consisted of a water-cooled copper crucible in which the constituent materials were placed, a conducting needle, and a sealable chamber. Metals were placed within the copper crucible, and the chamber was sealed and filled with argon gas. A current was run across the copper plate, generating a plasma beam used to melt the metals. Metals were repeatedly melted in the argon-filled chamber, with less than .5% sample mass loss. The newly formed compound was sealed in a partially evacuated, partially filled vycor tube of argon gas. To increase homogeneity, samples were annealed for 72 hours at 1123 K, just below the melting point of the samples. Samples were then quenched in cold water. Experimental samples were cut from larger buttons using a slow-speed diamond saw.

The physical properties of samples were then characterized. X-ray diffraction (XRD) measurements were used to find the structure and phase purity of samples. Measurements were performed at room temperature. XRD measurements were performed using a Scintag PAD-X1 Powder x-ray diffractometer, with a monochromatic Cu-K α 1 radiation source. PowderCell¹⁰ was used to determine crystalline structure and lattice parameters.

Samples magnetic properties were characterized using a physical property measurement system (PPMS) from Quantum Design, Inc. Measurements were performed over a range of temperatures, from 5 - 400K, at up to 50 kOe. Changes in magnetic entropy were found using the changing magnetic field at different temperatures using the Maxwell equation¹⁵:

$$\Delta S_M = - \int_0^H \left[\left(\frac{\partial M}{\partial T} \right)_H dH \right] \quad (1)$$

Results and Discussion

Using X-ray diffraction, the lattice parameters of our compound, and the program PowderCell¹⁰ we were able to confirm the compounds have Miller Indices that correspond to a cubic structure (Figure 1). These indices correspond to a L2₁ cubic structure, with a lattice parameter of 6.0634Å for the parent compound. A three dimensional representation of the crystal lattice of our compound can be found in Figure 2. A comparison of the X-ray diffraction reveals that copper doping has very little effect on the structure of the lattice, as can be seen by the consistency of peak locations across various doping amounts (Figure 1). Peak locations correspond to angles of alignment with the lattice, and are directly related to lattice structure. Lattice parameters, which correspond to the length of one side of the cube, for the various copper dopings were found (Table 1). There is only minor fluctuation in lattice parameter as copper is added, quantifying and confirming the relatively constant structure of the compounds.

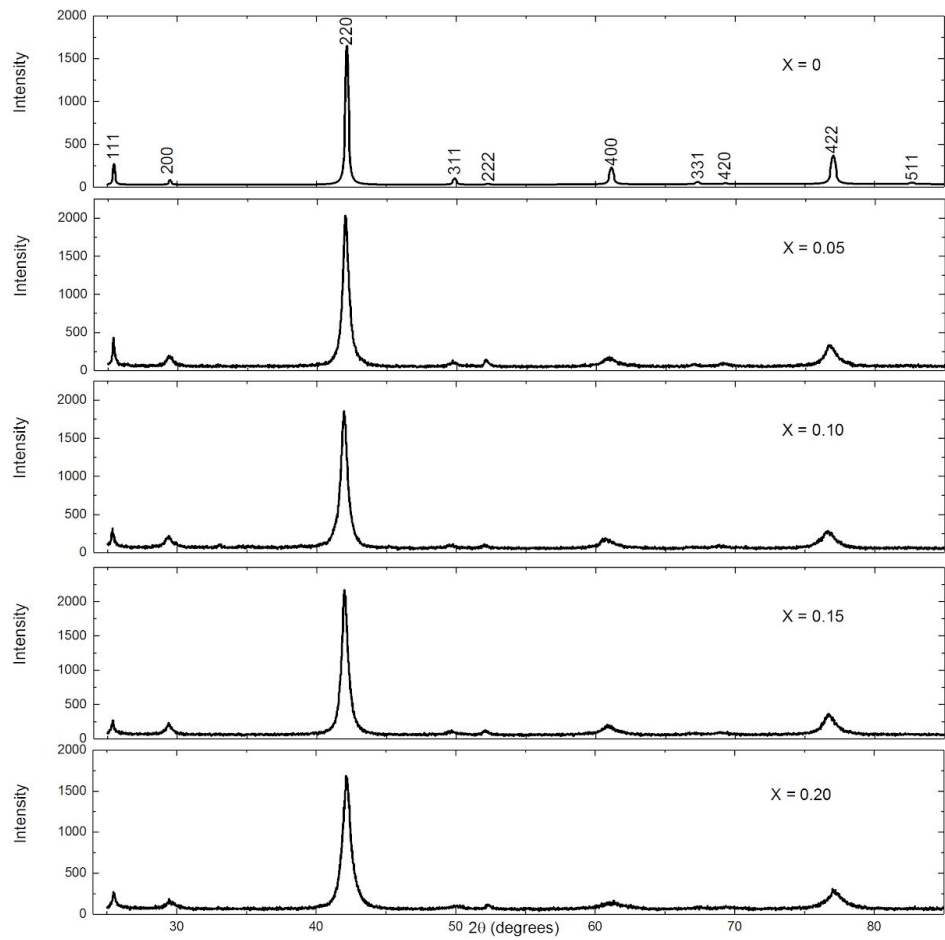


Figure 1: Results of X-Ray diffraction, created using Powder Cell. 2θ angles corresponding to peak intensities used to determine lattice structure, miller indices, and lattice parameters.

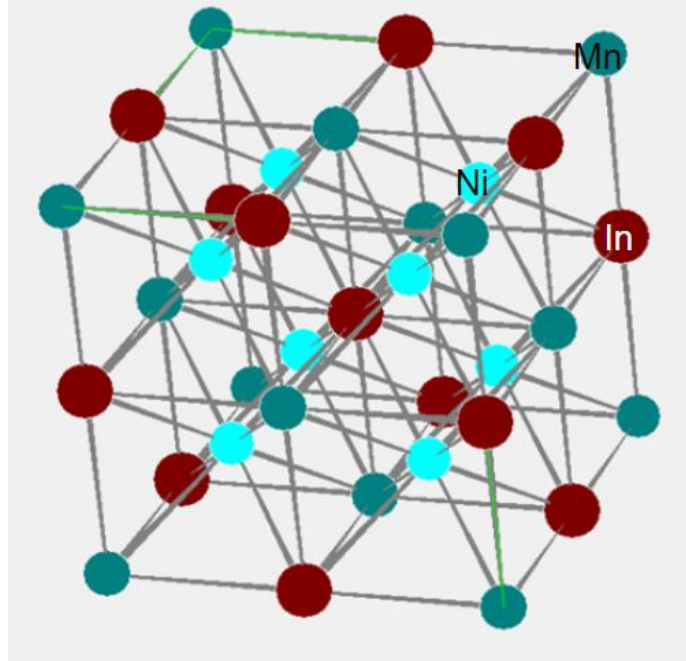


Figure 2: The cubic structure of our parent compound made using PowderCell⁶. This shows the relative positions of Nickel (light blue), Manganese (teal), and Indium (red).

X-Value	Lattice Parameter (Å)
0.00	6.0634
0.05	6.0733
0.10	6.0729
0.15	6.0813
0.20	6.0502

Table 1: The lattice parameter of the $\text{Ni}_2\text{Mn}_{1-x}\text{Cu}_x\text{In}$ as the copper doping occurs.

After the lattice structure of the compounds were characterized, the phase transition of each compound was determined. SOMT phase transitions are characterized by a lack of hysteresis when examining moment versus temperature. Raising and lowering the temperature of each compound produced identical moment values, confirming that there is no hysteresis present in our parent compound (Figure 3). An identical procedure was conducted on the copper doped samples, producing similar results (Figure 4). Since the materials are second order, they

do not undergo any physical lattice changes when they change from ferromagnetic to paramagnetic, and are thus not prone to corrosion.

As illustrated, the Curie temperature is the very point where a material loses its permanent magnetic properties, displayed by the randomly aligned dipole moments generated by electron spin in atoms^{18 19}. Therefore, the temperature at which the most dramatic change in moment occurs is the Curie temperature. Examination of each curve gives a rough estimate of T_C , and exact values can be determined by finding the point with the greatest magnitude first derivative. Figures 4 and 5 also show the Curie temperatures for each value of X, showing 313 K for the parent $X = 0$, 266 K for $X = 0.05$, 319 K for $X = 0.10$, 291 K for $X = 0.15$, and 252 K for $X = 0.20$. Data for the $X = 0.10$ sample displays an unexpected trend involving a plateau effect midway through its descent. The source of this plateau is unknown, and may be due to a measurement or sample preparation error. There are no prominent physical interpretations for the presented trend of $X = 0.10$. For practical use, Curie temperature should be as close to room temperature as possible. As for now the compound $X = 0.15$ with Curie temperature just two degrees lower than room temperature shows promise for application.

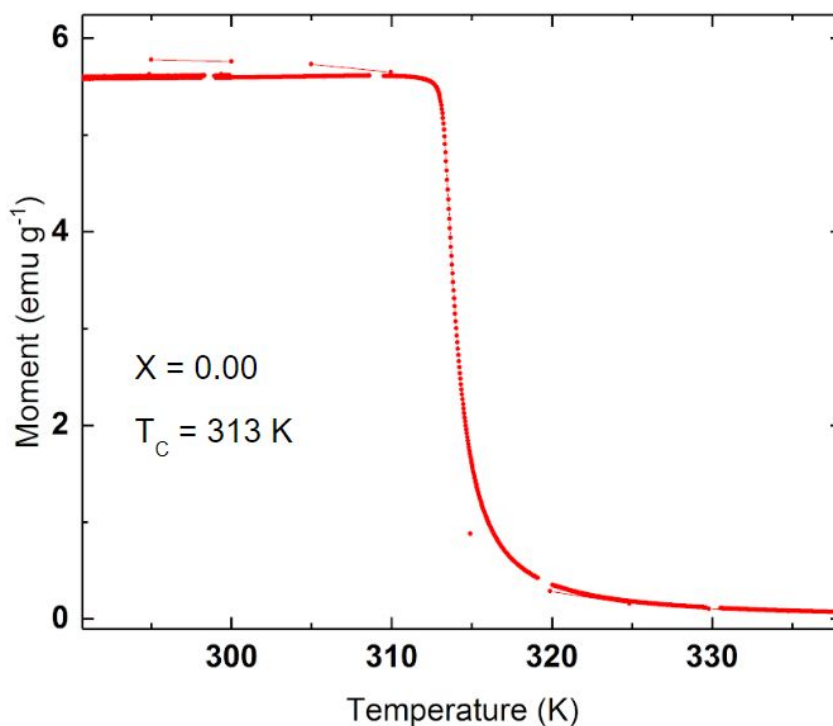


Figure 3: Moment versus temperature for parent compound Ni_2MnIn . Temperature was raised and lowered, with no hysteresis becoming evident, confirming a SOMT phase transition.

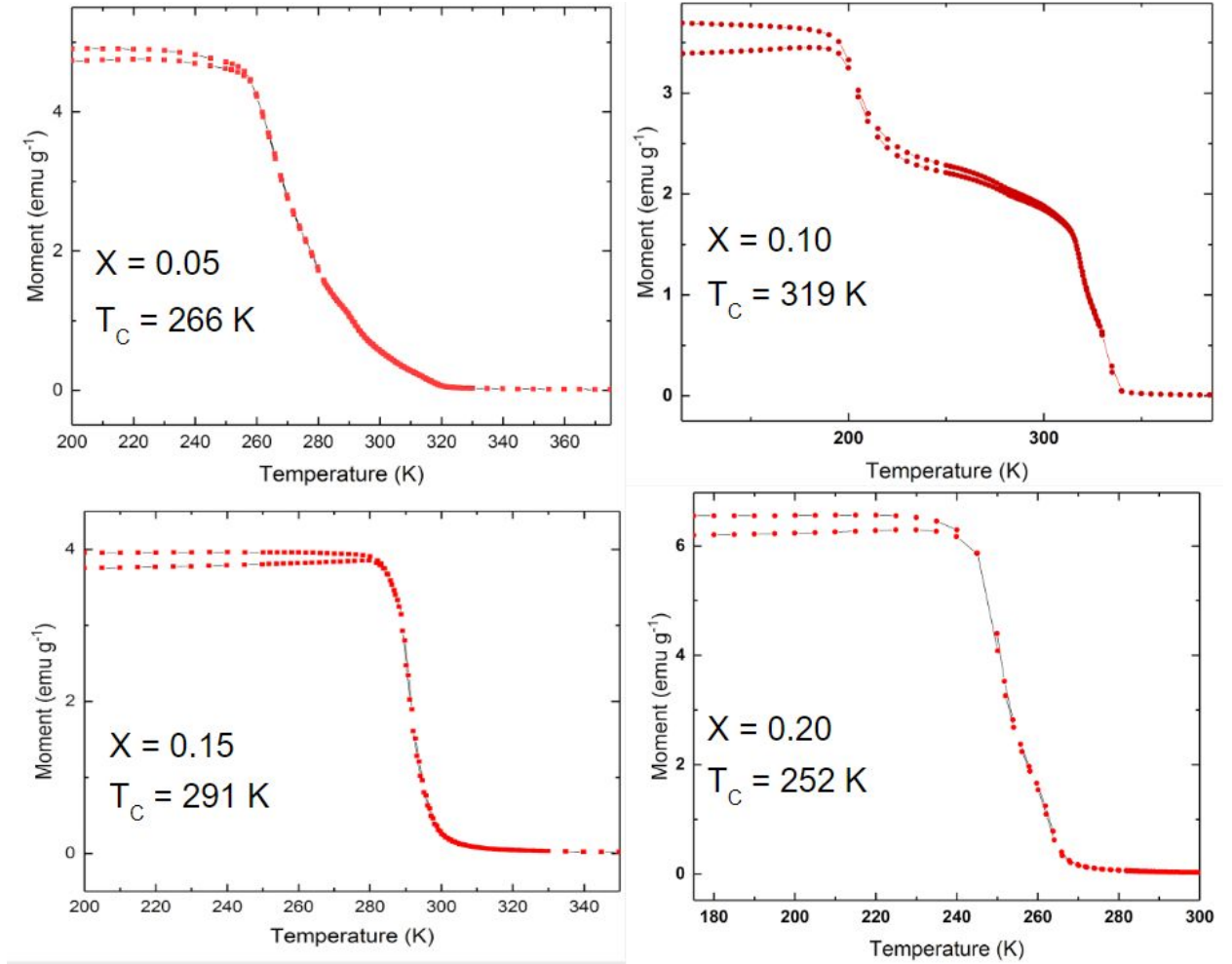


Figure 4: Moment versus temperature for various copper doping of Ni₂Mn_{1-x}Cu_xIn. Temperature was raised and lowered, with no hysteresis becoming evident for any compounds, confirming SOMT phase transitions for each. Curie temperatures were found at the points of greatest change in moment.

To further characterize the magnetic properties of the parent compound, a graph of magnetic moment versus magnetic field was created (Figure 5). This graph is meant to identify the relation between magnetic moment and a driven magnetic field. This graph confirms that the moment of the parent compound aligns with the magnetic field. Furthermore, a low moment hysteresis with a changing field may allow for more rapid cycling and better refrigeration.

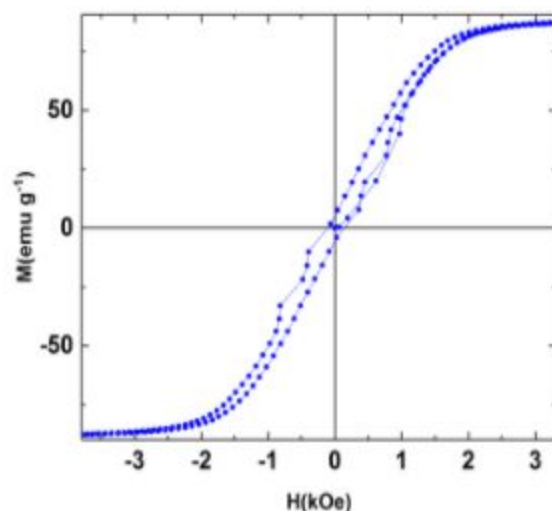


Figure 5: Magnetic moment loop as a function of the external magnetic field as the strength of the magnetic field is raised, lowered, and raised again for parent compound Ni_2MnIn . Demonstrates that the moment of the material aligns with the direction of the field.

To determine the usefulness of this set of compounds in magnetic refrigeration, a series of graphical analyses were performed. The first analysis necessary was the production of magnetic moment versus magnetic field over various temperatures. The parent compound was examined over a range of 240 K to 360 K (Figure 6). The copper doped compounds were examined over a range of 140 K to 380 K (Figure 7). Generally, as temperature increases, there is an overall decrease in magnetic moment and the magnetic moment becomes more dependent on field strength for all compounds examined.

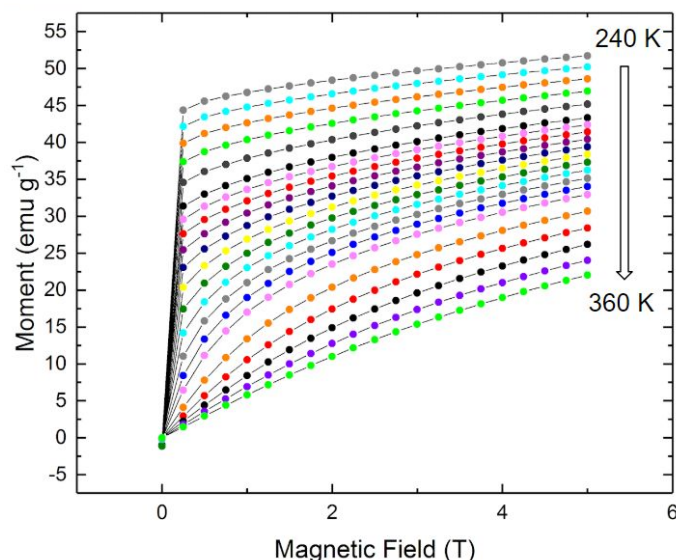


Figure 6: The magnetic moment as a function of magnetic field strength for parent compound Ni_2MnIn . Measurements were taken from 240-360 K. As temperature increases, magnetic moment becomes more dependent on field strength and generally decreases.

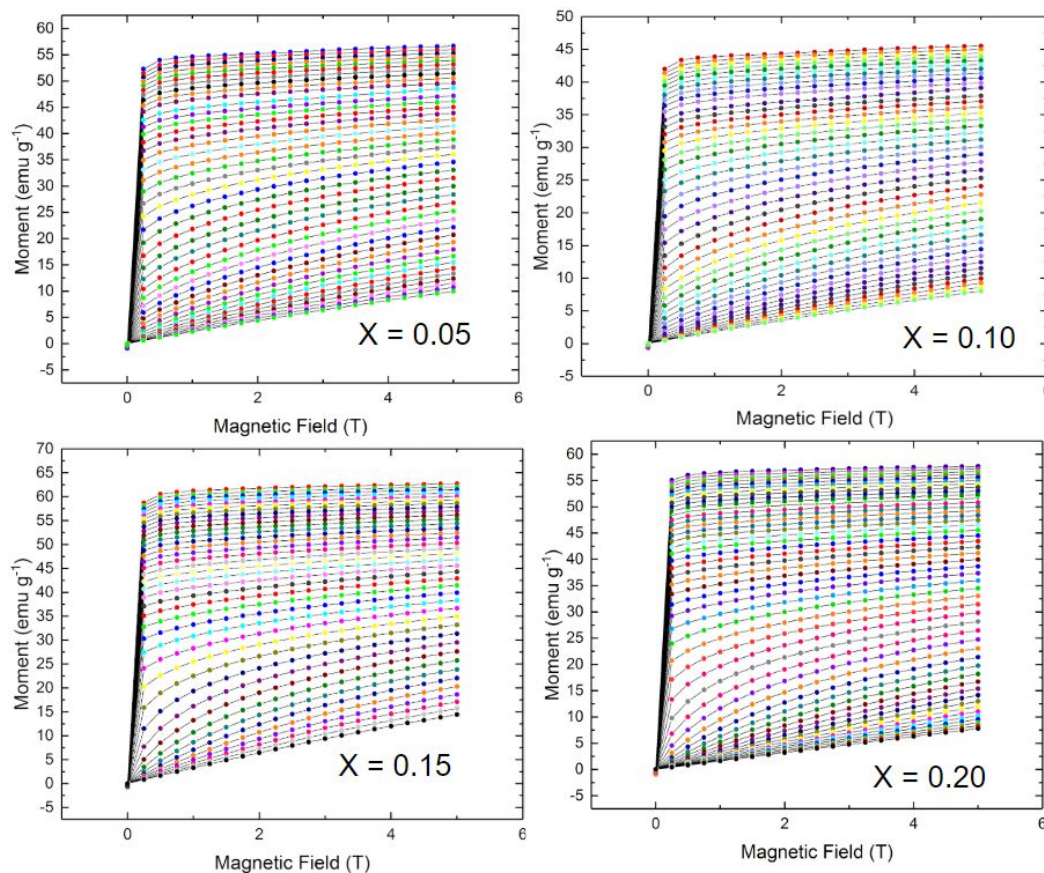


Figure 7: The magnetic moment as a function of magnetic field strength for various copper doping in $\text{Ni}_2\text{Mn}_{1-x}\text{Cu}_x\text{In}$. Measurements were taken from 140 (top) -380 (bottom) K. As temperature increases, magnetic moment becomes more dependent on field strength and generally decreases.

The space between each temperature in the multi-temp graph of moment and field can be integrated and used to generate a plot of the change in magnetic entropy versus temperature for various field strengths. The change in magnetic entropy for the parent compound can be found in Figure 8. The change in magnetic entropy for the copper doped substances can be found in Figure 9. Materials were examined in fields ranging from 1 T to 5 T. Notice that maximum entropy change approximately occurs at the Curie temperature of each material.

In turn, the area under the curve for the change in entropy versus temperature can be integrated at full width and half maximum value. The resulting values correspond to the refrigeration capacity of the material (R_C). This is an important metric in quantifying the usefulness of a material used in magnetic refrigeration. A summary table of these results can be found in Table 2. Refrigeration capacities were calculated for 2 T and 5 T fields for each material. These correspond to the most idealistic scenario (5 T) and a more realistic scenario in actual application in refrigeration (2 T). The highest refrigeration capacity is found in $x = .10$, followed by $x = .05$, then $x = .15$ for both magnetic fields.

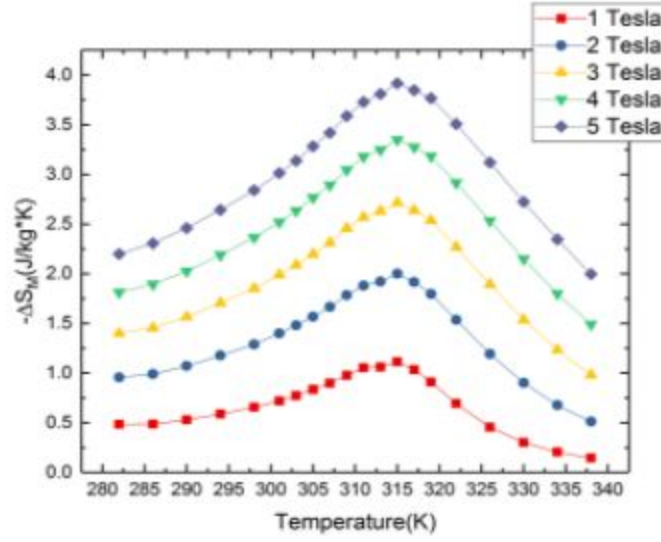


Figure 8: Change in magnetic entropy (ΔS_M) versus temperature for parent compound Ni_2MnIn at various external magnetic field strengths.

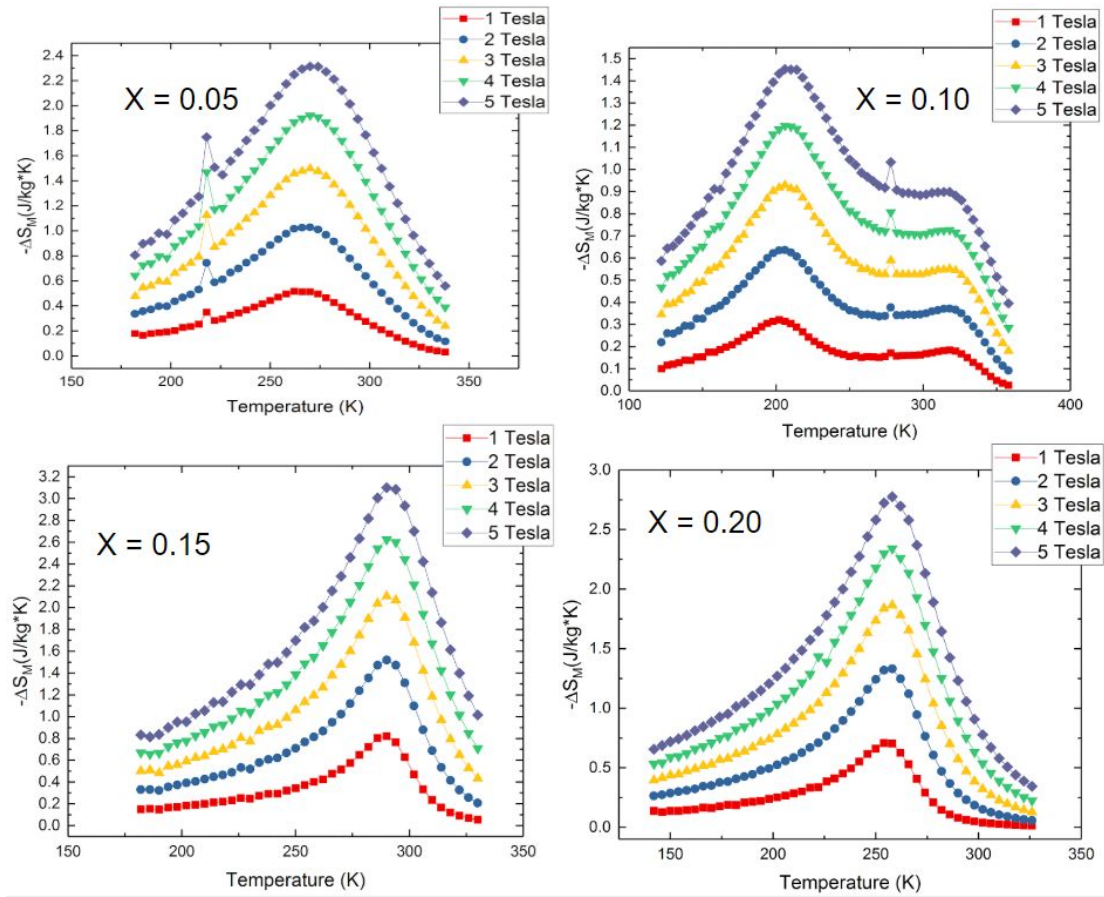


Figure 9: Change in magnetic entropy (ΔS_M) versus temperature for Cu doped $\text{Ni}_2\text{Mn}_{1-X}\text{Cu}_X\text{In}$ for various copper doping amounts at various external magnetic field strengths.

X-Value	R_C at 2 T (J Kg ⁻¹)	R_C at 5 T (J Kg ⁻¹)
0.00	55.553	167.432
0.05	71.828	191.887
0.10	78.868	203.625
0.15	60.241	170.396
0.20	57.240	160.172

Table 2: Refrigeration capacity (R_C) of our compounds in both the 2 T and 5 T fields. R_C was found by taking the integral of the Magnetic Entropy vs Temperature curves (Figures 9 and 10) at full width and half maximum height.

Previous research has found that Gd has a T_c of 319 K and a R_c of 203 J/kg²¹. However, Gd is rare and expensive. $Gd_{60}Al_{10}Mn_{30}$ has been found to have a R_C of 660 J/kg while Fe-doped Gd wires have a R_C of 748 J/kg at 5 T field^{22,26}; $Gd_{C(50+5x)}Al_{C(30-5x)}Co_{20}$ ($x = 0, 1, 2$)'s refrigeration capacity is 654 J/kg at 5T^{24,25} while a $Gd_{65}Mn_{25}Si_{10}$ -Gd composite has R_C values for multilayer and bulk composites of 724 and 617 J/kg ($\Delta m_0 H = 5T$), respectively; $Gd_5Ge_2Si_{2-x}Sn_x$ compounds, values of the order of 20 J kg⁻¹ K⁻¹ for $-\Delta S_T$ were obtained in as-cast samples when submitted to a magnetic field variation of 2 T²³. $LaFe_{11.4}Si_{1.6}$ has a T_c of 210 K and a R_c of 530 J/kg. $Ce_6Ni_2Si_3$ and $Fe_{48}Rh_{52}$ has Curie temperatures of 295 and 300 K respectively with a R_c of 700 J/kg and 500 J/kg²⁰. $Fe_{48}Rh_{52}$ is made up of more inexpensive materials but it is a first order phase transition compound so this is not practical for magnetic refrigeration. These data were for the previously made MCE materials and exhibit good refrigeration capacities; however, the compounds they use are fairly expensive compared to our compounds.

Conclusion

We have finished obtaining the data for our sample compounds, most of which exhibit expected behaviors. The consistent lattice parameters we obtained from X-ray diffraction showed the cubic structure of the compounds and their low variation in lattice structure. We also calculated curie temperature(T_c) and refrigeration capacity (R_C) for each sample. The T_c 's range from 252K to 319K; the R_C 's are generally optimal around $x = 0.10$ value under different magnetic field. Throughout our analysis, we saw a consistent trend that the optimal values seem to occur in the $x = 0.10$ compound. We did observe some strange behavior when looking at the Moment vs Temperature graphs. This could mean that our results are skewed since we found an optimal R_c . Re-examination of the $x = 0.10$ is necessary to help us understand if this is an error that is interfering with our results or if there is some physical interpretation for the anomaly. After looking through the literature, even if the data we found were correct, these materials were did not have as the same R_c as other researched compounds. There is some further analysis as our compound is more economically synthesized than many of the others with significantly higher R_c values. We also would like to conduct further research at levels around $x = 0.10$ to see if we can find an even better R_c value that still has a T_c near room temperature.

References

- [1] E.L.T. França, A.O. dos Santos, A.A. Coelho, L.M. da Silva. (2016). "Magnetocaloric effect of the ternary Dy, Ho and Er platinum gallides". *J. Mag. and Mag. Mat.* **401**. 1088–1092.
- [2] Brück, E. (2005). "Developments in magnetocaloric refrigeration". *J. of Phys. D: App. Phys.* **38** 23 R381.
- [3] Khovaylo, V. V.; Rodionova, V. V.; Shevyrtalov, S. N.; Novosad, V. (2014). "Magnetocaloric effect in "reduced" dimensions: Thin films, ribbons, and microwires of Heusler alloys and related compounds". *Physica status solidi* **251** 10 2104.
- [1] Nancy Hall. Second Law of Thermodynamics.
<https://www.grc.nasa.gov/www/k-12/airplane/thermo2.html> (2015)
- [2] Zion Market Research. Commercial Refrigeration Equipment Market size worth \$61.44 billion by 2021. (2017)
- [3] Smith, A. Who Discovered the Magnetocaloric Effect?
<https://doi.org/10.1140/epjh/e2013-40001-9> (2013)
- [4] Christine Thomas. Germanium Statistics and Information.
<https://minerals.usgs.gov/minerals/pubs/commodity/germanium/> (2018)
- [5] Maggie K., Kirsten S. The Periodic Table by Element Name.
<https://hobart.k12.in.us/ksms/PeriodicTable/abc.htm> (2005)
- [6] V. Franco, J.S. Blazquez, J.J. Ipus, J.Y. Law, L.M. Moreno-Ramirez, A. Conde. Magnetocaloric effect: From materials research to refrigeration devices. *Prog in Mat Sci.* **93** 11 232
- [7] Wang DH, Su ZH, Huang SL, Han Z, Zou WQ, Du, YW. The magnetic entropy changes in $Gd_{1-x}B_x$ alloys. *Solid State Communications* **131** 97 9
- [8] Wang DH, Su ZH, Huang SL, Han Z, Zou WQ, Du YW. The magnetic entropy changes in $Gd_{1-x}C_x$ alloys. *J Alloys Comp* **387** 6 8
- [9] V. K. Pecharsky and K.A. Gschneider, Jr. *Phys. Rev. Lett.* **78** 4494
- [10] https://www.bam.de/de/service/publikationen/powder_cell.htm for more information about Powder Cell; accessed 6 April 2018.
- [11] Harmon BN, Antonov VN. Electronic structure, optical, and magneto-optical properties of Gd-5(Si₂Ge₂) compound. *J Appl Phys* **91** 9815 20.
- [12] A. Planes, L Manosa, M. Acet. *J Phys Condens Matter* **21** 23 233201
- [13] Franco V, Blazquez JS, Conde A. Field dependence of the magnetocaloric effect in materials with a second order phase transition: a master curve for the magnetic entropy change. *Appl Phys Lett* **89** 222512.

- [14] Kuz'min MD. Factors limiting the operation frequency of magnetic refrigerators. *Appl Phys Lett* **90** 251916.
- [15] T. Hashimoto, T. Numasawa, M. Shino, and T. Okada, *Cryogenics* **21** 647
- [16] Jeffrey Brock, Mahmud Khan (2016). Large refrigeration capacities near room temperature in $\text{Ni}_2\text{Mn}_{1-x}\text{Cr}_x\text{In}$. *Journal of Magnetism and Magnetic Materials* **425** 1–5
- [17] Harmon BN, Antonov VN. Electronic structure, optical, and magneto-optical properties of $\text{Gd}_5(\text{Si}_2\text{Ge}_2)$ compound. *J Appl Phys* **91** 9815 20.
- [18] Levy, Robert A. (1968). *Principles of Solid State Physics*. Academic Press. ISBN 978-0124457508.
- [19] Fan, H. Y. (1987). *Elements of Solid State Physics*. Wiley-Interscience. ISBN 9780471859871.
- [20] Moreno-Ramírez LM, Blázquez JS, Law JY, Franco V, Conde A. Optimal temperature range for determining magnetocaloric magnitudes from heat capacity. *J Phys D: Appl Phys* **49** 495001.
- [21] Andrew Lee. Curie Temperature of Gadolinium.
<https://hypertextbook.com/facts/2004/AndrewLee.shtml> (2004)
- [22] Felicia Lau. Curie Temperature of Iron.
<https://hypertextbook.com/facts/2002/FeliciaLau.shtml> (2002)
- [23] A. Magnus G. Carvahlo, J. C. G. Tedesco, M. J. M. Pires. Large magnetocaloric effect and refrigerant capacity near room temperature in as-cast $\text{Gd}_5\text{Ge}_2\text{Si}_2-x\text{Sn}_x$ compounds. *Appl. Phys. Lett.* **102**, 192410
- [24] H. X. Shen, D. W. Xing, J. L. Sánchez Llamazares. Enhanced refrigerant capacity in Gd-Al-Co microwires with a biphasic nanocrystalline/ amorphous structure. *Appl. Phys. Lett.* **108** 092403
- [25] Jingshun Liu, Qixiang Wang, Mengjun Wu. Improving the refrigeration capacity of Gd-rich wires through Fe-doping. *J. of Alloys and Comps.* **711** 71-76
- [26] S. Gorsse, B. Chevalier, G. Orveillon. Magnetocaloric effect and refrigeration capacity in $\text{Gd}_{60}\text{Al}_{10}\text{Mn}_{30}$ nanocomposite. *Appl. Phys. Lett.* **92** 122501